

1 **Short Title:** Monocot ELF3 functions in dicots

2

3

4

5

6

7 **Corresponding Author:**

8

9 Dmitri A. Nusinow, Ph.D.

10 Assistant Member

11 Danforth Plant Science Center

12 975 N. Warson Rd.- Room 3030

13 St. Louis, MO 63132

14 (314)587-1489

15 [dmeter@danforthcenter.org](mailto:dmeter@danforthcenter.org)

16

17 **Cross-species complementation reveals conserved functions for EARLY FLOWERING 3**  
18 **between monocots and dicots**

19

20 He Huang, Malia A. Gehan, Sarah E. Huss, Sophie Alvarez<sup>2</sup>, Cesar Lizarraga, Ellen L.  
21 Gruebbling, John Gierer, Michael J. Naldrett<sup>2</sup>, Rebecca K. Bindbeutel, Bradley S. Evans, Todd  
22 C. Mockler, and Dmitri A. Nusinow\*

23

24 Donald Danforth Plant Science Center, St. Louis, MO, 63132, USA (H.H., M.A.G., S.A., C.L.,  
25 J.G., M.J.N., R.K.B., B.S.E., T.C.M., D.A.N.)

26 Webster University, Webster Groves, MO, 63119, USA (S.E.H.)

27 Saint Louis University, St. Louis, MO, 63103, USA (E.L.G.)

28

29 **One Sentence Summary:**

30 Orthologs of a key circadian clock component ELF3 from grasses functionally complement the  
31 Arabidopsis counterpart at the molecular and physiological level, in spite of high sequence  
32 divergence.

33

34 **Footnotes:**

35

36 H.H., M.A.G., T.C.M., and D.A.N. conceived the project; T.C.M., B.S.E. and D.A.N. supervised  
37 the experiments; H.H., M.A.G., S.E.H., S.A., C.L., E.L.G., J.G., M.J.N., R.K.B. and D.A.N.  
38 performed the experiments; H.H., M.A.G., S.E.H., S.A., C.L., M.J.N. and D.A.N. analyzed the  
39 data; H.H., M.A.G., and D.A.N. wrote the manuscript. All authors edited the manuscript.

40

41 <sup>1</sup>This work was supported by the National Science Foundation (NSF) grant (IOS-1456796) to  
42 D.A.N., the NSF (DBI-0922879) grant for acquisition of the LTQ-Velos Pro Orbitrap LC-  
43 MS/MS, the U.S. Department of Energy grants ([DE-SC0006627](#), [DE-SC0012639](#), and [DE-](#)  
44 [SC0008769](#)) to T.C.M. and the NSF-Plant Genome grant (IOS-1202682) to M.A.G.

45 <sup>2</sup> Present addresses: University of Nebraska-Lincoln, Lincoln, NE, 68588, USA

46 \*Corresponding author email: [meter@danforthcenter.org](mailto:meter@danforthcenter.org)

47

48

49 **ABSTRACT**

50

51 Plant responses to the environment are shaped by external stimuli and internal signaling  
52 pathways. In both the model plant *Arabidopsis thaliana* and crop species, circadian clock factors  
53 have been identified as critical for growth, flowering and circadian rhythms. Outside of *A.*  
54 *thaliana*, however, little is known about the molecular function of clock genes. Therefore, we  
55 sought to compare the function of *Brachypodium distachyon* and *Setaria viridis* orthologs of  
56 *EARLY FLOWERING3*, a key clock gene in *A. thaliana*. To identify both cycling genes and  
57 putative ELF3 functional orthologs in *S. viridis*, a circadian RNA-seq dataset and online query  
58 tool (Diel Explorer) was generated as a community resource to explore expression profiles of  
59 *Setaria* genes under constant conditions after photo- or thermo-entrainment. The function of  
60 *ELF3* orthologs from *A. thaliana*, *B. distachyon*, and *S. viridis* were tested for complementation  
61 of an *elf3* mutation in *A. thaliana*. Despite comparably low sequence identity versus AtELF3  
62 (less than 37%), both monocot orthologs were capable of rescuing hypocotyl elongation,  
63 flowering time and arrhythmic clock phenotypes. Molecular analysis using affinity purification  
64 and mass spectrometry to compare physical interactions also found that BdELF3 and SvELF3  
65 could be integrated into similar complexes and networks as AtELF3, including forming a  
66 composite evening complex. Thus, we find that, despite 180 million years of separation, BdELF3  
67 and SvELF3 can functionally complement loss of *ELF3* at the molecular and physiological level.

68

## 69 INTRODUCTION

70

71 Plants have developed sophisticated signaling networks to survive and thrive in diverse  
72 environments. Many plant responses are shaped, in part, by an internal timing mechanism known  
73 as the circadian clock, which allows for the coordination and anticipation of daily and seasonal  
74 variation in the environment (Greenham and McClung, 2015). Circadian clocks, which are  
75 endogenous oscillators with a period of approximately 24 hours, are critical for regulating the  
76 timing of physiology, development, and metabolism in all domains of life (Bell-Pedersen et al.,  
77 2005; Doherty and Kay, 2010; Edgar et al., 2012; Harmer, 2009; Wijnen and Young, 2006). In  
78 plants and blue-green algae, circadian clocks provide an experimentally observable adaptive  
79 advantage by synchronizing internal physiology with external environmental cues (Dodd et al.,  
80 2005; Ouyang et al., 1998; Woelfle et al., 2004). Currently, circadian oscillators are best  
81 understood in the reference plant *Arabidopsis thaliana*, in which dozens of clock or clock-  
82 associated components have been identified using genetic screens and non-invasive, luciferase-  
83 based oscillating reporters (Hsu and Harmer, 2014; Nagel and Kay, 2012). These morning-,  
84 afternoon-, and evening-phased clock oscillators form multiple interconnected transcription-  
85 translation feedback loops and compose a complex network (Hsu and Harmer, 2014; Pokhilko et  
86 al., 2012). The *A. thaliana* circadian clock regulates a significant portion of physiology,  
87 including photosynthesis, growth, disease resistance, starch metabolism, and phytohormone  
88 pathways (Covington et al., 2008; Graf et al., 2010; Harmer et al., 2000; Michael et al., 2008;  
89 Wang et al., 2011b), with up to 30% of gene expression under circadian control (Covington et  
90 al., 2008; Michael et al., 2008).

91 Within the *Arabidopsis* clock network, a tripartite protein complex called the evening complex  
92 (EC) is an essential component of the evening transcription loop (Huang and Nusinow, 2016b).  
93 The EC consists of three distinct proteins, EARLY FLOWERING 3 (ELF3), EARLY  
94 FLOWERING 4 (ELF4) and LUX ARRHYTHMO (LUX, also known as PHYTOCLOCK1),  
95 with transcript and protein levels peaking in the evening (Doyle et al., 2002; Hazen et al., 2005;  
96 Hicks et al., 2001; Nusinow et al., 2011; Onai and Ishiura, 2005). The EC plays a critical role in  
97 maintaining circadian rhythms, by repressing expression of key clock genes (Dixon et al., 2011;  
98 Helfer et al., 2011; Herrero et al., 2012; Kolmos et al., 2011; Mizuno et al., 2014). Loss-of-

99 function mutation of any EC component in *A. thaliana* results in arrhythmicity of the circadian  
100 clock and causes excessive cellular elongation and early flowering regardless of environmental  
101 photoperiod (Doyle et al., 2002; Hazen et al., 2005; Hicks et al., 2001; Khanna et al., 2003; Kim  
102 et al., 2005; Nozue et al., 2007; Nusinow et al., 2011; Onai and Ishiura, 2005).

103  
104 In *A. thaliana*, ELF3 directly interacts with ELF4 and LUX, functioning as a scaffold to bring  
105 ELF4 and LUX together (Herrero et al., 2012; Nusinow et al., 2011). Additional protein-protein  
106 interaction studies and tandem affinity purification coupled with mass spectrometry (AP-MS)  
107 have identified many ELF3-associating proteins and established ELF3 as a hub of a complex  
108 protein-protein interaction network, which consists of key components from the circadian clock  
109 pathway and light signaling pathways (Huang et al., 2016a; Huang and Nusinow, 2016b; Liu et  
110 al., 2001; Yu et al., 2008). In this network, ELF3 directly interacts with the major red light  
111 photoreceptor phytochrome B (phyB), and CONSTITUTIVE PHOTOMORPHOGENIC 1  
112 (COP1), which is an E3 ubiquitin ligase required for proper regulation of photomorphogenesis  
113 and also interacts with phyB (Liu et al., 2001; Yu et al., 2008). The physical interaction among  
114 ELF3, phyB, and COP1, together with recruitment of direct interacting proteins to the network,  
115 provides biochemical evidence for cross-talk between circadian clock and light signaling  
116 pathways (Huang and Nusinow, 2016b). Although much work does translate from *A. thaliana* to  
117 other plant species, interaction between ELF3 and other proteins have yet to be tested in species  
118 outside *A. thaliana*. Whether evening complex-like protein assemblages or a similar ELF3-  
119 containing protein-protein interaction network exists in species outside *A. thaliana* is an  
120 interesting question to ask.

121  
122 Identification and characterization of clock genes in diverse plant species has revealed that many  
123 clock components are broadly conserved (Filichkin et al., 2011; Khan et al., 2010; Lou et al.,  
124 2012; Song et al., 2010). Furthermore, comparative genomics analysis has found that circadian  
125 clock components are selectively retained after genome duplication events, suggestive of the  
126 importance of their role in maintaining fitness (Lou et al., 2012). Recently, mutant alleles of  
127 *ELF3* were identified associated with the selection of favorable photoperiodism phenotypes in  
128 several crops, such as pea, rice, soybean and barley (Faure et al., 2012; Lu et al., 2017;

129 Matsubara et al., 2012; Saito et al., 2012; Weller et al., 2012; Zakhrebekova et al., 2012). These  
130 findings are consistent with the reported functions of *A. thaliana* ELF3 in regulating the  
131 photoperiodic control of growth and flowering (Hicks et al., 2001; Huang and Nusinow, 2016b;  
132 Nozue et al., 2007; Nusinow et al., 2011). However, opposed to the early flowering phenotype  
133 caused by *elf3* mutants in *A. thaliana*, pea, and barley (Faure et al., 2012; Hicks et al., 2001;  
134 Weller et al., 2012), loss of function mutation of the rice or soybean *ELF3* ortholog results in  
135 delayed flowering (Lu et al., 2017; Saito et al., 2012), suggesting ELF3-mediated regulation of  
136 flowering varies in different plant species. The molecular mechanisms underlying this difference  
137 have not been thoroughly elucidated.

138  
139 *Brachypodium distachyon* is a C3 model grass closely related to wheat, barley, oats, and rice.  
140 *Setaria viridis*, is a C4 model grass closely related to maize, sorghum, sugarcane, and other  
141 bioenergy grasses. Both grasses are small, transformable, rapid-cycling plants with recently  
142 sequenced genomes, making them ideal model monocots for comparative analysis with  
143 *Arabidopsis* (Bennetzen et al., 2012; Brutnell et al., 2010). Computational analysis of *B.*  
144 *distachyon* has identified putative circadian clock orthologs (Higgins et al., 2010), including  
145 *BdELF3*. However, no such comparative analysis has been done systematically in *S. viridis* to  
146 identify putative orthologs of circadian clock genes. Therefore, we generated a RNA-seq time-  
147 course dataset to analyze the circadian transcriptome of *S. viridis* after either photo- or thermo-  
148 entrainment and developed an online gene-expression query tool (Diel Explorer) for the  
149 community. We found that the magnitude of circadian regulated genes in *S. viridis* is similar to  
150 other monocots after photo-entrainment, but much less after thermal entrainment. We further  
151 analyzed the functional conservation of SvELF3, together with previously reported BdELF3, by  
152 introducing both ELF3 orthologs into *A. thaliana elf3* mutant for physiological and biochemical  
153 characterization. We found that *B. distachyon* and *S. viridis* ELF3 can complement the hypocotyl  
154 elongation, flowering time and circadian arrhythmia phenotypes caused by the *elf3* mutation in  
155 *A. thaliana*. Furthermore, AP-MS analyses found that *B. distachyon* and *S. viridis* ELF3 were  
156 integrated into a similar protein-protein interaction network *in vivo* as their *A. thaliana*  
157 counterpart. Our data collectively demonstrated the functional conservation of ELF3 among *A.*

158 *thaliana*, *B. distachyon* and *S. Viridis* is likely due to the association with same protein partners,  
159 providing insights of how ELF3 orthologs potentially function in grasses.

160

## 161 **RESULTS**

162

### 163 **Identifying and cloning ELF3 orthologs from *B. distachyon* and *S. viridis***

164

165 ELF3 is a plant-specific nuclear protein with conserved roles in flowering and the circadian  
166 clock in multiple plant species (Faure et al., 2012; Herrero et al., 2012; Liu et al., 2001; Lu et al.,  
167 2017; Matsubara et al., 2012; Saito et al., 2012; Weller et al., 2012; Zakhrabekova et al., 2012).  
168 To identify ELF3 orthologs in monocots, we used the protein sequence of *Arabidopsis thaliana*  
169 ELF3 (AtELF3) to search the proteomes of two model monocots *Brachypodium distachyon* and  
170 *Setaria viridis* using BLAST (Altschul et al., 1990). Among the top hits, we identified a  
171 previously reported ELF3 homolog in *B. distachyon* (*Bradi2g14290.1*, *BdELF3*) (Calixto et al.,  
172 2015; Higgins et al., 2010) and two putative *ELF3* homologous genes *Sevir.5G206400.1*  
173 (referred as *SvELF3a*) and *Sevir.3G123200.1* (referred as *SvELF3b*) in *S. viridis*. We used  
174 Clustal Omega (<http://www.ebi.ac.uk/Tools/msa/clustalo/>) to conduct multiple sequence  
175 alignments of comparing protein sequences of ELF3 orthologs with that of AtELF3 (Sievers et  
176 al., 2011). *BdELF3*, *SvELF3a* and *SvELF3b* encode proteins with similar identity compared to  
177 AtELF3 (34.7–36.8%) (**Supplemental Figure S1**). When compared to *BdELF3*, *SvELF3b* was  
178 74.3% identical while *SvELF3a* was 57.4% identical (**Supplemental Figure S1**). Therefore, to  
179 maximize the diversity of ELF3 sequences used in this study, we cloned full length cDNAs  
180 encoding *BdELF3* and *SvELF3a*.

181

### 182 **Diel Explorer of *S. viridis* circadian data**

183

184 In *Arabidopsis*, ELF3 cycles under diel and circadian conditions (constant condition after  
185 entrainment) with a peak phase in the evening (Covington et al., 2001; Hicks et al., 2001;  
186 Nusinow et al., 2011). We queried an available diurnal time course expression dataset for *B.*  
187 *distachyon* from the DIURNAL website, and found that *BdELF3* expression cycles under diel



188 conditions (LDHH, 12 h light / 12 h dark cycles with constant temperature), but not under  
189 circadian conditions in available data (LDHC-F or LDHH-F, **Supplemental Figure S2**)  
190 (Filichkin et al., 2011; Mockler et al., 2007). Also different from *AtELF3*, transcript levels of  
191 *BdELF3* accumulate at dawn rather than peak in the evening (**Supplemental Figure S2**) when  
192 grown under diel conditions, suggesting different regulations on *ELF3* expression between  
193 monocot and dicot plants. Neither diel nor circadian expression data for *S. viridis* was available.  
194 Therefore, we generated RNA-seq time-course data to examine *SvELF3* expression as well as the  
195 circadian expression of other clock orthologs after both photocycle and thermocycle entrainment.  
196 In addition, we developed the Diel Explorer tool  
197 (<http://shiny.bioinformatics.danforthcenter.org/diel-explorer/>) to query and visualize *S. viridis*  
198 circadian-regulated gene expression (**Supplemental Figure S3**). 48,594 *S. viridis* transcripts are  
199 represented in the two datasets entrained under either photocycles (LDHH-F) or thermocycles  
200 (LLHC-F). With Diel Explorer users can manually enter a list of transcript identifiers, gene  
201 ontology (GO) terms, or gene orthologs, plot gene expression, and download data. Alternatively,  
202 users can upload files of transcript identifiers or gene orthologs, and/or filter the datasets by  
203 entrainment, phase, or significance cut-offs. Data and graphs can be downloaded directly using  
204 Diel Explorer. The tool serves as a community resource that can be expanded to include other  
205 circadian or diurnal data in the future. The underlying code is available on Github  
206 (<https://github.com/danforthcenter/diel-explorer>).

207  
208 Under photoperiod entrainment (LDHH-F), 5,585 of the 48,594 *S. viridis* transcripts are  
209 circadian regulated (Bonferroni-adjusted P-Value < 0.001). This proportion of photoperiod-  
210 entrained circadian genes (~11.5%) is similar to maize (10.8%), rice (12.6%), and poplar  
211 (11.2%) data sets, but much smaller than the approximately 30% reported for *A. thaliana*  
212 (Covington et al., 2008; Filichkin et al., 2011; Khan et al., 2010). Under thermocycle  
213 entrainment (LLHC-F), 582 of the 48,594 *S. viridis* transcripts are circadian regulated.  
214 Therefore, only ~1.2% of *S. viridis* transcripts are circadian cycling under thermocycle  
215 entrainment. The ~10-fold reduction in circadian cycling genes between photocycle and  
216 thermocycle entrainment (**Supplemental Figure S4**) is interesting considering that there was  
217 less than 1% difference in the number of genes with a circadian period between photocycle and



218 thermocycle entrainment in C3 monocot rice (*Oryza japonica*) (Filichkin et al., 2011). The  
219 reduction in cycling genes between the two entrainment conditions in *S. viridis* compared to *O.*  
220 *japonica* is an indication that circadian regulation could vary greatly among monocots. Also, the  
221 difference in number of cycling genes between monocots and dicots may represent a significant  
222 reduction of the role of the circadian clock between these lineages.

223

224 In addition to the overall reduction in circadian genes, the phase with the most number of cycling  
225 genes was ZT18 after light entrainment (LDHH-F; **Supplemental Figure S4**), but ZT12 with  
226 temperature entrainment (LLHC-F; **Supplemental Figure S4**), which is consistent with previous  
227 studies that have found significant differences in temperature and light entrainment of the  
228 circadian clock (Boikoglou et al., 2011; Michael et al., 2008; Michael et al., 2003). There are 269  
229 genes that are considered circadian-regulated and are cycling under both LDHH-F and LLHC-F  
230 conditions (Bonferroni Adjusted P-Value < 0.001). The list of 269 genes that overlap between  
231 photocycle and thermocycle entrainment includes best matches for Arabidopsis core clock  
232 components *TIMING OF CAB EXPRESSION 1* (*TOC1*, *AT5G61380.1*; *Sevir.1G241000.1*),  
233 *LATE ELONGATED HYPOCOTYL* (*LHY*, *AT1G01060*; *Sevir.6G053100.1*), and *CCA1*-like gene  
234 *REVEILLE1* (*RVE1*, *AT5G17300.1*; *Sevir.1G280700.1*). However, putative *S. viridis* orthologs of  
235 *TOC1*, *LHY*, and *RVE1* all have different circadian phases under LDHH entrainment compared  
236 to LLHC entrainment (**Figure 1**). In fact, the majority (233/269) of overlapping circadian genes  
237 in *S. viridis* have a distinct circadian phase under thermocycle compared to photocycle entrainment  
238 (**Supplemental Figure S4**). We also found that putative orthologs of *PSEUDO-RESPONSE*  
239 *REGULATOR 7* (*PRR7*, *AT5G02810*; *Sevir.2G456400.1*; related to *OsPRR73* (Murakami et  
240 al., 2003)) and *LUX ARRHYTHMO* (*LUX*, *AT3G46640*; *Sevir.5G474200.1*) cycle significantly  
241 under LDHH-F but not LLHC-F conditions (**Figure 1**). Neither *SvELF3a* nor *SvELF3b* cycle  
242 under circadian conditions after photo- or thermo-entrainment (**Figure 1**), similar to *ELF3*  
243 orthologs in *B. distachyon* (**Supplemental Figure S2**) (Mockler et al., 2007) and *O. sativa*  
244 (Filichkin et al., 2011). This is different from *AtELF3*, which continues to cycle under constant  
245 condition after either photo- or thermos-entrainment (**Supplemental Figure S5**) (Mockler et al.,  
246 2007). The difference in expression of these putative orthologs between *A. thaliana* and

247 monocots *S. viridis*, *B. distachyon*, and *O. sativa*, suggest that the architecture of the circadian  
248 clock may have significant differences in response to environmental cues in these two species.

249

### 250 **BdELF3 and SvELF3 rescue growth and flowering defects in *Arabidopsis elf3* mutant**

251

252 Although the circadian expression pattern of *B. distachyon ELF3* and *S. viridis ELF3* is different  
253 from that of *A. thaliana ELF3*, it is still possible that the ELF3 orthologs have conserved  
254 biological functions. To test this, we sought to determine if BdELF3 or SvELF3a could  
255 complement the major phenotypic defects of the *elf3* mutant in *A. thaliana*, namely hypocotyl  
256 elongation, time to flowering, or circadian rhythmicity. To this end, we constitutively expressed  
257 *BdELF3*, *SvELF3a* (hereafter referred as *SvELF3*) and *AtELF3* cDNAs by the *35S Cauliflower*  
258 *mosaic virus* promoter in the *A. thaliana elf3-2* mutant expressing a *LUCIFERASE* reporter  
259 driven by the promoter of *CIRCADIAN CLOCK ASSOCIATED 1 (CCA1)* (*elf3-2 [CCA1:LUC]*)  
260 (Pruneda-Paz et al., 2009). All three ELF3 coding sequences were fused to a C-terminal His<sub>6</sub>-  
261 3xFlag affinity tag (HFC), which enables detection by western blotting and identification of  
262 protein-protein interaction by affinity purification and mass spectrometry (AP-MS) (Huang et al.,  
263 2016a). After transforming these constructs, we identified and selected two biologically  
264 independent transgenic lines with a single insertion of each At/Bd/SvELF3-HFC construct.  
265 Western blot analysis using FLAG antibodies detected the expression of all ELF3-HFC fusion  
266 proteins (**Supplemental Figure S6**).

267

268 Next, we asked if expressing At/Bd/SvELF3-HFC fusion proteins could rescue the mutation  
269 defects caused by *elf3-2*. When plants are grown under light/dark cycles (12 hour light: 12 hour  
270 dark), *elf3-2* mutant plants elongate their hypocotyls much more than wild type plants ( $4.75 \pm 0.48$   
271 mm vs.  $1.95 \pm 0.27$  mm, respectively.  $\pm$  = standard deviation) (**Figure 2**). The long hypocotyl  
272 defect in *elf3-2* was effectively suppressed by expressing either *AtELF3*, or *ELF3* orthologs  
273 (*BdELF3* or *SvELF3a*) (**Figure 2**). These data show that the monocot *ELF3* orthologs function  
274 similarly to *A. thaliana ELF3* in the regulation of hypocotyl elongation in seedlings.

275

276 In addition to regulating phenotypes in seedlings, ELF3 also functions in adult plants to suppress  
277 the floral transition. Loss-of-function in Arabidopsis *ELF3* results in an early flowering  
278 phenotype regardless of day-length (Hicks et al., 2001; Liu et al., 2001; Zagotta et al., 1992). To  
279 determine how monocot ELF3 orthologs compared to *A. thaliana* ELF3 in flowering time  
280 regulation, we compared flowering responses under long day conditions among wild type, *elf3-2*,  
281 and *elf3-2* transgenic lines expressing *AtELF3*, *BdELF3*, or *SvELF3* (At/Bd/SvELF3-HFC).  
282 Constitutive over-expression of *AtELF3* led to a delay in flowering in long days (**Figure 3**) as  
283 previously observed (Liu et al., 2001). Similarly, constitutive expression of *BdELF3* or *SvELF3*  
284 caused plants to flower significantly later than the *elf3* mutants. These data show that all *ELF3*  
285 orthologs can function to repress the rapid transition to flowering of the *elf3* mutation when  
286 constitutively expressed in adult plants.

287

### 288 **BdELF3 and SvELF3 restore the circadian rhythmicity in Arabidopsis *elf3* mutant**

289

290 ELF3 is a key component of the *A. thaliana* circadian clock and is critical for maintaining the  
291 periodicity and amplitude of rhythms as shown using the *CCA1* promoter driven luciferase  
292 reporter (CCA:LUC) (Covington et al., 2001; Hicks et al., 1996; Nusinow et al., 2011). To  
293 determine if *BdELF3* or *SvELF3a* could rescue the arrhythmic phenotype of the *elf3* mutation,  
294 we analyzed the rhythms of the *CCA1::LUC* reporter under constant light conditions after diel  
295 entrainment (12 hours light: 12 hours dark at constant 22 °C). Relative amplitude error (RAE)  
296 analysis found that 100% of wild type and nearly all of the three *elf3-2* transgenic lines  
297 expressing *AtELF3*, *BdELF3* (*BdELF3* #3 was 87.5% rhythmic), and *SvELF3* were rhythmic,  
298 while only 37.5 % of the *elf3-2* lines had measurable rhythms (RAE < 0.5) (**Supplemental**  
299 **Figure S7**). Comparison of average period length found that the *AtELF3* expressing lines  
300 completely rescued the period and amplitude defects in the *elf3* mutant (**Figure 4A** and **4D**). The  
301 *SvELF3* and *BdELF3* lines also rescued the amplitude defect (**Figure 4B** and **4C**), but their  
302 period was longer than wild type (compare  $23.21 \pm 0.59$  hours for wild type to *BdELF3* #2=  
303  $27.68 \pm 0.86$  hours, *BdELF3* #3=  $26.39 \pm 1.01$  hours, *SvELF3* #2=  $24.47 \pm 0.50$  hours, *SvELF3*  
304 #3=  $24.32 \pm 0.34$  hours, and *elf3-2*=  $31.27 \pm 1.93$  hours,  $\pm$  = standard deviation, **Figure 4D**). In

305 summary, these data show that expression of any of the ELF3 orthologs is sufficient to recover  
306 the amplitude and restore rhythms of the *CCA1::LUC* reporter.

307

308 **BdELF3 and SvELF3 are integrated into a similar protein-protein interaction network in**  
309 ***A. thaliana***

310

311 Despite relatively low sequence conservation at the protein level, the *ELF3* orthologs can  
312 complement a wide array of *elf3* phenotypes (**Figures 2 to 4**). As ELF3 functions within the  
313 evening complex (EC) in Arabidopsis, which also contains the transcription factor LUX and the  
314 DUF-1313 domain containing protein ELF4 (Herrero et al., 2012; Nusinow et al., 2011), we  
315 reasoned that the monocot *ELF3* orthologs may also be able to bind to these proteins when  
316 expressed in *A. thaliana*. To determine if a composite EC could be formed, we tested if BdELF3  
317 or SvELF3a could directly interact with AtLUX or AtELF4 in a yeast two-hybrid assay. Similar  
318 to AtELF3 (Nusinow et al., 2011), both BdELF3 and SvELF3a directly interact with both  
319 AtELF4 and the C-terminal portion of AtLUX (**Figure 5**). We cannot conclude that whether  
320 monocot ELF3 orthologs are also able to interact with the N-terminal AtLUX, since this  
321 fragment auto-activated the reporter gene in the yeast two-hybrid assay (**Figure 5**).

322

323 ELF3 functions not only as the scaffold of the EC, but also as a hub protein in a protein-protein  
324 interaction network containing multiple key regulators in both the circadian clock and light  
325 signaling pathways (Huang et al., 2016a; Huang and Nusinow, 2016b). We hypothesize that  
326 BdELF3 and SvELF3 could rescue many of the defects of the *elf3* mutant because both monocot  
327 versions were integrated into the same protein-protein interaction network. To test this  
328 hypothesis, we used affinity purification and mass spectrometry (AP-MS) to identify the proteins  
329 that co-precipitate with monocot ELF3s when expressed in *A. thaliana*. AP-MS on two  
330 biological replicates for each sample with the above-mentioned independent insertion lines were  
331 included for each ELF3 ortholog. For comparison, the same AP-MS experiment was done with  
332 one of the 35S promoter-driven AtELF3-HFC transgenic lines (AtELF3-2). To detect specific  
333 co-precipitating proteins, we manually removed commonly identified contaminant proteins from  
334 plant affinity purifications and mass spectrometry experiments (Van Leene et al., 2015), and

335 proteins identified from a control transgenic line expressing GFP-His<sub>6</sub>-3xFlag described  
336 previously (Huang et al., 2016a) (**Table 1**, the full list of identified proteins can be found in  
337 **Supplemental Table S2**).

338  
339 We have previously reported proteins that co-precipitated with ELF3 driven from its native  
340 promoter using a similar AP-MS methodology (Huang et al., 2016a). When using the 35S  
341 promoter driven AtELF3 transgenic line, we were able to generate a curated list of 22 proteins  
342 that specifically co-precipitate with AtELF3, including all previously identified proteins, such as  
343 all five phytochromes, PHOTOPERIODIC CONTROL OF HYPOCOTYL1 (PCH1) (Huang et  
344 al., 2016c), and COP1 (**Table 1**). In addition, we also identified LIGHT-REGULATED WD 2  
345 (LWD2) and SPA1-RELATED 4 (SPA4) as now co-precipitating with AtELF3. These additional  
346 interactions may be a result of a combination of altered seedling age, expression level of the  
347 ELF3 bait, or tissue-specificity of expression due to these purifications are from tissues where  
348 the epitope-tagged transgene is constitutively over-expressed. However, since LWD2 is a known  
349 component of the circadian clock (Wu et al., 2008) and SPA4 is a known component of the  
350 COP1-SPA complex (Zhu et al., 2008), these interactions are likely to be relevant.

351  
352 In comparing the list of BdELF3 and SvELF3 co-precipitated proteins with that of AtELF3, we  
353 found that neither SvELF3 nor BdELF3 co-precipitated SPA2 and SPA4, components of the  
354 COP1-SPA complex. In addition, SvELF3 did not co-precipitate MUT9-LIKE KINASE1, a  
355 kinase with roles in chromatin modification and circadian rhythms as AtELF3 did (Huang et al.,  
356 2016a; Wang et al., 2015). However, BdELF3 and SvELF3 associated with most of the proteins  
357 found in AtELF3 AP-MS (20 out of 22 for BdELF3, 19 out of 22 for SvELF3), in at least one of  
358 the replicate purifications from each monocot ortholog AP-MS. Therefore our data suggest that  
359 BdELF3 and SvELF3 are integrated into a similar protein-protein interaction network as  
360 AtELF3, which likely underlies their ability of broadly complementing *elf3* mutants.

361

## 362 **DISCUSSION**

363

364 Recent work in diverse plant species has found that the circadian clock plays critical roles in  
365 regulating metabolism, growth, photoperiodism, and other agriculturally important traits (Bendix  
366 et al., 2015; McClung, 2013; Shor and Green, 2016). While the relevance of the circadian clock  
367 to plant fitness is unquestioned, it is unclear if the circadian clock components have conserved  
368 function among different plant species. This is particularly true for the majority of clock proteins,  
369 whose biological functions are currently poorly understood at the molecular level (Hsu and  
370 Harmer, 2014). Also, the divergent modes of growth regulation and photoperiodism between  
371 monocots and dicots suggest that the clock evolved to have altered roles in regulating these  
372 physiological responses between lineages (Matos et al., 2014; Poire et al., 2010; Song et al.,  
373 2014). Here we asked if orthologs of ELF3 from two monocots could complement any of the  
374 loss-of-function phenotypes in the model dicot plant *A. thaliana*. In this study we found that  
375 ELF3 from either *B. distachyon* or *S. viridis* could complement the hypocotyl elongation, early  
376 flowering, and arrhythmic clock phenotype of the *elf3* mutant in *A. thaliana*, despite the  
377 variations in protein sequences and evolutionary divergence between monocot and dicot plants.  
378 These data suggest that monocot ELF3s can functionally substitute for *A. thaliana* ELF3, albeit  
379 with varying efficacy. Since monocot and dicot ELF3 are largely different in the protein  
380 sequences, functional conservation of ELF3 orthologs also leads to the next open question of  
381 identifying the functional domains within ELF3.

382  
383 Previously, comparison of ELF3 homologs has identified at least five conserved regions that may  
384 be important for function (**Supplemental Figure S1**) (Liu et al., 2001; Saito et al., 2012; Weller  
385 et al., 2012). Our multiple sequence alignments also show that at least two regions of AtELF3,  
386 namely the N-terminus (AA 1~49) and one middle region (AA 317~389) share many conserved  
387 residues with ELF3 orthologs in grasses (**Supplemental Figure S1**). These regions fall within  
388 known fragments that are sufficient for binding to phyB (Liu et al., 2001), COP1 (Yu et al.,  
389 2008), or ELF4 (Herrero et al., 2012). Consistent with the hypothesis that these conserved  
390 regions are critical for proper ELF3 function, a single amino acid substitution (A362V) within  
391 this middle region results in defects of ELF3 nuclear localization and changes in the circadian  
392 clock period (Anwer et al., 2014). In addition, our protein-protein interaction study and AP-MS  
393 analysis show that both monocot ELF3 can form composite ECs (**Figure 5**) and that all three



394 ELF3 homologs interact with an almost identical set of proteins *in vivo* (**Table 1**), further  
395 suggesting that one or more of the conserved regions may mediate the binding between ELF3  
396 and its known interacting proteins. Furthermore, the similar pool of ELF3 interacting proteins  
397 identified by Bd/SvELF3 AP-MS suggests that the overall conformation of ELF3 ortholog  
398 proteins is conserved and that similar complexes and interactions with ELF3 orthologs may form  
399 in monocot species. However, whether these interactions form *in planta* and have the same effect  
400 on physiology is unclear. For example, *S. viridis* data generated here and public data for *B.*  
401 *distachyon* and *O. sativa*, showed that ELF3 does not cycle under circadian conditions, which  
402 differs from Arabidopsis. Further, different from the fact that the clock plays a key role in  
403 regulating elongation in *A. thaliana* (Nozue et al., 2007), the circadian clock has no influence on  
404 growth in C3 model grass *B. distachyon*, despite robust oscillating expression of putative clock  
405 components (Matos et al., 2014). Similarly, ELF3 from rice (*Oryza sativa*) and soybean  
406 promotes flowering and senescence (Lu et al., 2017; Saito et al., 2012; Sakuraba et al., 2016;  
407 Yang et al., 2013; Zhao et al., 2012), while in *A. thaliana*, ELF3 represses these responses (Liu et  
408 al., 2001; Sakuraba et al., 2014; Zagotta et al., 1992), which suggests significant rewiring of  
409 ELF3 regulated photoperiodic responses of flowering between short-day (rice/soybean) and  
410 long-day (*A. thaliana*) plants. Alternatively, ELF3 may form distinct interactions and complexes  
411 in monocot species that were not identified in our trans-species complementation analysis.  
412 Clearly, further work is required to understand ELF3 function in monocots beyond the studies  
413 presented here.

414  
415 In addition to the molecular characterization of ELF3, our analysis of circadian-regulated genes  
416 in *S. viridis* after photo- and thermo-entrainment found significant differences in the behavior of  
417 the clock when compared to other monocots. Although the number of circadian regulated genes  
418 is comparable to studies done in corn and rice after photo-entrainment (between 10-12%)  
419 (Filichkin et al., 2011; Khan et al., 2010), we found that very few genes (~1%) continue to cycle  
420 after release from temperature entrainment in *S. viridis* (**Supplemental Figure S4**) when  
421 compared to rice (~11%) (Filichkin et al., 2011). This may reflect a fundamental difference in  
422 how the clock interfaces with temperature between these monocot species. Furthermore,  
423 proportions of circadian regulated genes upon photo-entrainment in all three monocot plants



424 **(Supplement Figure S4)** (Filichkin et al., 2011; Khan et al., 2010) are much smaller than the  
425 approximately 30% reported for *A. thaliana* (Covington et al., 2008), suggesting the divergence  
426 of clock functions through evolution or domestication. Further comparisons of circadian  
427 responses among monocots or between monocots and dicots will help to determine the molecular  
428 underpinning of these differences.

429

430 In summary, we find that BdELF3 and SvELF3 form similar protein complexes *in vivo* as  
431 AtELF3, which likely allows for functional complementation of loss-of-function of *elf3* despite  
432 relatively low sequence conservation. We also present an online query tool, Diel Explorer that  
433 allows for exploration of circadian gene expression in *S. viridis*, which illustrate fundamental  
434 differences in clock function among monocots and between monocots and dicots. Collectively,  
435 this work is a first step toward functional understanding of the circadian clock in two model  
436 monocots, *S. viridis* and *B. distachyon*.

437

## 438 **MATERIALS AND METHODS**

439

### 440 **Plant materials and growth conditions**

441

442 For *A. thaliana*, wild type (Columbia-0) and *elf3-2* plants carrying the CCA1::LUC reporter were  
443 described previously (Nusinow et al., 2011; Pruneda-Paz et al., 2009). Seeds were surface  
444 sterilized and plated on 1/2x Murashige and Skoog (MS) basal salt medium with 0.8% agar + 1%  
445 (w/v) sucrose. After 3 days of stratification, plates were placed horizontally in a Percival  
446 incubator (Percival Scientific, Perry, IA), supplied with  $80 \mu\text{mol m}^{-2} \text{sec}^{-1}$  white light and set to a  
447 constant temperature of 22°C. Plants were grown under 12 h light / 12 h dark cycles (12L:12D)  
448 for 4 days (for physiological experiments) or for 10 days (for AP-MS) before assays.

449

450 For *S. viridis* circadian expression profiling by RNA-seq, seeds were stratified for 5 days at 4°C  
451 before being moved to entrainment conditions. Plants were grown under either LDHH or LLHC  
452 (L: light, D: dark, H: hot, C: cold) entrainment condition, and then sampled for RNA-seq in  
453 constant light and constant temperature (32°C) conditions (F, for free-running) every 2 hours for

454 48 hours. Light intensity was set to  $400 \mu\text{mol m}^{-2} \text{sec}^{-1}$  white light. In LDHH-F, stratified *S.*  
455 *viridis* seeds were grown for 10 days under 12L:12D and constant temperature ( $32^{\circ}\text{C}$ ) before  
456 sampling in constant light and constant temperature. In LLHC-F, stratified *S. viridis* seeds were  
457 grown for 10 days under constant light conditions and cycling temperature conditions 12 h at  
458  $32^{\circ}\text{C}$  (subjective day) / 12 h at  $22^{\circ}\text{C}$  (subjective night) before sampling in constant conditions.  
459 Two experimental replicates were collected for each entrainment condition.

460

### 461 **Setaria circadian RNA-seq**

462

463 The second leaf from the top of seventeen *S. viridis* plants was selected for RNA-seq sampling at  
464 each time point for each sampling condition. Five replicate samples were pooled after being  
465 ground in liquid nitrogen and resuspended in lithium chloride lysis binding buffer (Wang et al.,  
466 2011a). RNA-seq libraries from leaf samples were constructed according to the previous  
467 literature (Wang et al., 2011a) with one major modification. Rather than extracting RNA then  
468 mRNA from ground leaf samples (Wang et al., 2011a), mRNA was extracted directly from  
469 frozen ground leaf samples similar to the method described in (Kumar et al., 2012), except that  
470 two additional rounds of wash, binding, and elution steps after treatment with EDTA were  
471 necessary to remove rRNA from samples. mRNA quantity was assessed using a Qubit with a  
472 Qubit RNA HS Kit and mRNA quality was assessed using a Bioanalyzer and Plant RNA PiCO  
473 chip. 96 library samples were multiplexed 12 per lane, for a total of 8 lanes of Illumina HiSeq  
474 2000 sequencing. Paired end 101 bp Sequencing was done at MOgene (St. Louis, MO). Raw  
475 data and processed data can be found on NCBI's Gene Expression Omnibus (GEO; (Barrett et  
476 al., 2013; Edgar et al., 2002)) and are accessible with identification number GSE97739  
477 (<https://www.ncbi.nlm.nih.gov/geo/query/acc.cgi?acc=GSE97739>).

478

479 RNA-seq data was trimmed with BBTools (v36.20) using parameters: ktrim=r k=23 mink=11  
480 hdist=1 tpe tbo ktrim=l k=23 mink=11 hdist=1 tpe tbo qtrim=rl trimq=20 minlen=20 (Bushnell,  
481 2016). Any parameters not specified were run as default. Before trimming we had 1,814,939,650  
482 reads with a mean of 18,905,621 reads per sample and a standard deviation of 2,875,187. After  
483 trimming, we have 1,646,019,593 reads with a mean of 17,146,037 reads per sample and a

484 standard deviation of 2,411,061. Kallisto (v 0.42.4; (Bray et al., 2016)) was used to index the  
485 transcripts with the default parameters and the *S. viridis* transcripts fasta file (Sviridis\_311\_v1.1)  
486 from Phytozome (Goodstein et al., 2012). The reads were quantified with parameters:-t 40 -b  
487 100. Any parameters not specified were run as default. Kallisto output was formatted for  
488 compatibility with JTKCycle (v3.1; (Hughes et al., 2010)) and circadian cycles were detected.  
489 To query the *S. viridis* expression data we developed Diel Explorer. The tool can be found at  
490 <http://shiny.bioinformatics.danforthcenter.org/diel-explorer/>. Underlying code for Diel Explorer  
491 is available on Github (<https://github.com/danforthcenter/diel-explorer>).

492

### 493 **Plasmid constructs and generation of transgenic plants**

494

495 Coding sequences (without the stop codon) of *AtELF3* (AT2G25930) and *SvELF3a*  
496 (*Sevir.5G206400.1*) were cloned into the pENTR/D-TOPO vector (ThermoFisher Scientific,  
497 Waltham, MA), verified by sequencing and were recombined into the pB7HFC vector (Huang et  
498 al., 2016a) using LR Clonease (ThermoFisher Scientific, Waltham, MA ). Coding sequence of  
499 *BdELF3* (*Bradi2g14290.1*) was submitted to the U.S. Department of Energy Joint Genome  
500 Institute (DOE-JGI), synthesized by the DNA Synthesis Science group, and cloned into the  
501 pENTR/D-TOPO vector. Sequence validated clones were then recombined into pB7HFC as  
502 described above. The pB7HFC-At/Bd/SvELF3 constructs were then transformed into *elf3-2*  
503 [*CCA1::LUC*] plants by the floral dip method (Zhang et al., 2006). Homozygous transgenic  
504 plants were validated by testing luciferase bioluminescence, drug resistance, and by PCR-based  
505 genotyping. All primers used in this paper were listed in **Supplemental Table S1**.

506

### 507 **Hypocotyl and flowering time measurement**

508

509 20 seedlings of each genotype were arrayed and photographed with a ruler for measuring  
510 hypocotyl length using the ImageJ software (NIH) (Schneider et al., 2012). The procedure was  
511 repeated three times. For measuring flowering time, 12 plants of each genotype were placed in a  
512 random order and were grown under the long day condition (light : dark = 16 : 8 hours). The  
513 seedlings were then observed every day at 12:00 PM; the date on which each seedling began

514 flowering, indicated by the growth of a ~1 cm inflorescence stem, was recorded along with the  
515 number of rosette leaves produced up to that date. ANOVA analysis with Bonferroni correction  
516 was measured using GraphPad Prism version 6.00 (GraphPad Software, La Jolla California  
517 USA, [www.graphpad.com](http://www.graphpad.com)).

518

### 519 **Circadian assays in *A. thaliana***

520

521 Seedlings were transferred to fresh 1/2x MS plates after 5 days of entrainment under the  
522 12L:12D condition and sprayed with sterile 5 mM luciferin (Gold Biotechnology, St. Louis, MO)  
523 prepared in 0.1% (v/v) Triton X-100 solution. Sprayed seedlings were then imaged in constant  
524 light ( $70 \mu\text{mol m}^{-2} \text{sec}^{-1}$ , wavelengths 400, 430, 450, 530, 630, and 660 set at intensity 350  
525 (Heliospectra LED lights, Göteborg, Sweden)). Bioluminescence was recorded after a 120-180s  
526 delay to diminish delayed fluorescence (Gould et al., 2009) over 5 days using an ultra-cooled  
527 CCD camera (Pixis 1024B, Princeton Instruments) driven by Micro-Manager software (Edelstein  
528 et al., 2010; Edelstein et al., 2014). The images were processed in stacks by Metamorph software  
529 (Molecular Devices, Sunnyvale, CA), and rhythms determined by fast Fourier transformed non-  
530 linear least squares (FFT-NLLS) (Plautz et al., 1997) after background subtraction using the  
531 interface provided by the Biological Rhythms Analysis Software System 3.0 (BRASS) available  
532 at <http://www.amillar.org>.

533

### 534 **Yeast two-hybrid analysis**

535

536 Yeast two-hybrid assays were carried out as previously described (Huang et al., 2016a). In brief,  
537 the DNA binding domain (DBD) or activating domain (AD)-fused constructs were transformed  
538 using the Li-Ac transformation protocol (Clontech) into *Saccharomyces cerevisiae* strain Y187  
539 (MAT $\alpha$ ) and the AH109 (MAT $\alpha$ ), respectively. Two strains of yeast were then mated to generate  
540 diploid with both DBD and AD constructs. Protein-protein interaction was tested in diploid yeast  
541 by replica plating on CSM –Leu –Trp –His media supplemented with extra Adenine (30mg/L  
542 final concentration) and 2mM 3-Amino-1,2,4-triazole (3AT). Pictures were taken after 4-day

543 incubation at 30 °C. All primers used for cloning plasmid constructs were listed in  
544 **Supplemental Table S1.**

545

#### 546 **Protein extraction and western blotting**

547

548 Protein extracts were made from 10-day-old seedlings as previously described (Huang et al.,  
549 2016a) and loaded 50 µg to run 10% SDS-PAGE. For western blots, all of the following primary  
550 and secondary antibodies were diluted into PBS + 0.1% Tween and incubated at room  
551 temperature for 1 hour: anti-FLAG®M2-HRP (Sigma, A8592, diluted at 1:10,000) and anti-  
552 Rpt5-rabbit (ENZO Life Science, BML-PW8245-0025, diluted at 1:5000) and anti-Rabbit-HRP  
553 secondary antibodies (Sigma, A0545, diluted at 1:10,000).

554

#### 555 **Affinity purification and mass spectrometry**

556

557 Protein extraction methods and protocols for AP-MS were described previously (Huang et al.,  
558 2016a; Huang et al., 2016b; Huang and Nusinow, 2016a; Huang et al., 2016c)}. In brief,  
559 transgenic seedlings carrying the At/Bd/SvELF3-HFC constructs were grown under 12L:12D  
560 conditions for 10 days and were harvested at dusk (ZT12). 5 grams of seedlings were needed per  
561 replicate to make protein extracts, which underwent tandem affinity purification utilizing the  
562 FLAG and His epitopes of the fusion protein. Purified samples were reduced, alkylated and  
563 digested by trypsin. The tryptic peptides were then injected to an LTQ-Orbitrap Velos Pro  
564 (ThermoFisher Scientific, Waltham, MA) coupled with a U3000 RSLCnano HPLC  
565 (ThermoFisher Scientific, Waltham, MA) with settings described previously (Huang et al.,  
566 2016a).

567

#### 568 **AP-MS data analysis**

569

570 Data analysis was done as previously described (Huang et al., 2016a). The databases searched  
571 were TAIR10 database (20101214, 35,386 entries) and the cRAP database  
572 (<http://www.thegpm.org/cRAP/>). Peptide identifications were accepted if they could be

573 established at greater than 95.0% probability and the Scaffold Local FDR was <1%. Protein  
574 identifications were accepted if they could be established at greater than 99.0% probability as  
575 assigned by the Protein Prophet algorithm (Keller et al., 2002; Nesvizhskii et al., 2003). A full  
576 list of all identified proteins (reporting total/exclusive unique peptide count and percent  
577 coverage) can be found in **Supplemental Table S2**. The mass spectrometry proteomics data  
578 have been deposited to the ProteomeXchange Consortium (Vizcaino et al., 2014) via the PRIDE  
579 partner repository with the dataset identifier PXD006352 and 10.6019/PXD006352.

580

581

## 582 **Supplemental Data**

583 **Supplemental Table S1.** List of all primers used.

584 **Supplemental Table S2.** A full list of At/Bd/SvELF3 associated proteins identified from AP-  
585 MS.

586 **Supplemental Figure S1.** Multiple sequence alignments of ELF3 orthologs

587 **Supplemental Figure S2.** Diel and circadian expression of *BdELF3* from the DIURNAL  
588 database.

589 **Supplemental Figure S3.** Example of the Diel Explorer interface.

590 **Supplemental Figure S4.** Summary of circadian regulated genes in *S. viridis*.

591 **Supplemental Figure S5.** Circadian expression of selected *A. thaliana* clock genes from the  
592 DIURNAL database.

593 **Supplemental Figure S6.** Anti-FLAG western of ELF3 transgenic lines used for  
594 complementation analysis.

595 **Supplemental Figure S7.** Relative Amplitude Error vs period plots of transgenic *elf3-2* plants  
596 expressing At/Bd/SvELF3.

597

**Table 1. Proteins co-purified with ELF3 orthologs from AP-MS**

AGI number	Protein Name	Molecular Weight	Exclusive Unique Peptide Count/Percent Coverage <sup>a</sup>									
			AtELF3		SvELF3 #2		SvELF3 #3		BdELF3 #2		BdELF3 #3	
			rep1	rep2	rep1	rep2	rep1	rep2	rep1	rep2	rep1	rep2
n/a	AtELF3-HFC	84 kDa	20/36%	19/31%	—	—	—	—	—	—	—	—
n/a	SvELF3-HFC	87 kDa	—	—	19/40%	29/48%	22/42%	33/54%	—	—	—	—
n/a	BdELF3-HFC	86 kDa	—	—	—	—	—	—	25/42%	26/43%	21/35%	19/33%
AT2G18790	phyB	129 kDa	23/37%	24/37%	31/54%	28/42%	32/50%	30/45%	22/34%	22/33%	24/40%	24/37%
AT5G35840	phyC	124 kDa	22/29%	23/29%	27/37%	32/39%	27/37%	33/42%	20/24%	18/22%	19/23%	22/27%
AT5G43630	TZP	91 kDa	14/21%	12/17%	13/23%	20/33%	13/22%	24/36%	12/18%	13/19%	14/20%	14/22%
AT4G18130	phyE	123 kDa	11/16%	19/27%	12/18%	18/23%	11/19%	17/24%	6/7%	10/14%	14/19%	13/18%
AT2G16365.2	PCH1 <sup>b</sup>	51 kDa	9/25%	9/25%	9/30%	14/43%	11/36%	16/49%	9/26%	9/28%	11/32%	11/32%
AT2G46340	SPA1	115 kDa	8/14%	7/9%	2/2%	4/8%	2/3%	4/9%	—	—	6/8%	5/6%
AT3G42170 <sup>c</sup>	DAYSLEEPER	79 kDa	8/19%	5/11%	—	7/16%	—	12/27%	3/7%	4/8%	2/4%	—
AT2G32950	COP1	76 kDa	8/16%	9/17%	6/17%	4/8%	3/6%	5/12%	1/2%	2/4%	6/11%	4/8%
AT3G22380	TIC	165 kDa	5/5%	5/5%	4/4%	12/12%	3/3%	15/15%	4/4%	3/3%	1/1%	1/1%
AT4G11110	SPA2	115 kDa	5/11%	6/12%	—	—	—	—	—	—	—	—
AT2G40080	ELF4	12 kDa	4/50%	4/50%	3/42%	5/68%	4/60%	4/60%	4/50%	4/50%	5/68%	5/68%
AT1G09340 <sup>c</sup>	CRB	43 kDa	4/16%	3/12%	1/4%	1/4%	1/4%	4/18%	1/4%	1/4%	—	—
AT3G13670	MLK4	79 kDa	3/10%	3/13%	—	—	—	1/2%	6/21%	3/10%	3/11%	5/13%
AT5G61380	TOC1	69 kDa	2/4%	2/4%	2/5%	—	3/7%	—	—	—	1/2%	1/2%
AT1G53090	SPA4	89 kDa	2/6%	5/14%	—	—	—	—	—	—	—	—
AT5G18190	MLK1	77 kDa	2/12%	2/11%	—	—	—	—	2/14%	2/14%	2/11%	2/11%
AT3G26640	LWD2	39 kDa	2/21%	1/21%	—	1/16%	—	2/22%	3/27%	1/16%	—	—
AT1G12910	LWD1	39 kDa	2/21%	3/30%	2/21%	4/31%	1/17%	2/21%	2/22%	2/19%	0/11%	0/11%
AT4G16250	phyD	129 kDa	1/10%	1/11%	2/12%	1/12%	3/15%	2/12%	2/11%	1/10%	2/14%	2/12%
AT1G09570	phyA	125 kDa	1/1%	1/1%	7/11%	5/5%	7/11%	2/2%	—	2/2%	6/7%	3/4%



AT2G25760	MLK3	76 kDa	1/5%	1/6%	—	1/4%	—	1/4%	3/13%	2/9%	2/9%	2/9%
AT3G03940	MLK2	78 kDa	1/8%	1/8%	—	1/7%	—	0/2%	3/20%	2/13%	3/13%	1/9%
AT3G46640	LUX	35 kDa	1/3%	1/3%	0/10%	3/19%	0/10%	3/23%	1/3%	1/3%	1/3%	2/11%
AT1G17455	ELF4-L4	13 kDa	—	—	—	—	—	—	1/23%	1/23%	—	—
AT1G72630	ELF4-L2	13 kDa	—	1/11%	—	1/13%	—	—	1/22%	1/22%	1/22%	1/11%

Proteins co-purified with ELF3 orthologs (AtELF3, SvELF3 and BdELF3, with C-terminal His6-3xFLAG tag) were identified from affinity purification coupled with mass spectrometry (AP-MS) analyses using 12L:12D grown, 10-day-old transgenic plants (in *elf3-2 null* mutant backgrounds) harvested at ZT12.

<sup>a</sup> All listed proteins match 99% protein threshold, minimum number peptides of 2 and peptide threshold as 95%. Proteins not matching the criteria were marked with "—".

<sup>b</sup> Percent coverage for PCH1 is calculated using protein encoded by *At2g16365.2*

<sup>c</sup> These proteins have been noted as frequently identified proteins in AP-MS experiments (see Van Leene, 2015).

## 598 **FIGURE LEGENDS**

599

600 **Figure 1.** Circadian expression profiles of putative *S. viridis* clock components from Diel  
601 Explorer using time-course RNA-seq data. *S. viridis* plants were entrained by either photocycle  
602 (LDHH) or thermocycle (LLHC), followed by being sampled every 2 hours for 48 hours under  
603 constant temperature and light conditions (Free-Running; F) to generate time-course RNA-seq  
604 data. Mean values of Transcripts per Kilobase Million (TPM) from two experimental replicates  
605 for each timepoints per gene were plotted.

606

607 **Figure 2.** ELF3 orthologs suppress hypocotyl elongation defects in *elf3-2*. The hypocotyls of 20  
608 seedlings of wild type, *elf3-2* mutant, AtELF3 *elf3-2*, BdELF3 *elf3-2*, and SvELF3 *elf3-2* (two  
609 independent transgenic lines for each ELF3 ortholog) were measured at 4 days after germination  
610 under 12-hour light :12-hour dark growth conditions at 22 °C. Upper panel shows representative  
611 seedlings of each genotype, with scale bar equal to 5 mm. Mean and 95% confidence intervals  
612 are plotted as crosshairs. This experiment was repeated three times with similar results. ANOVA  
613 analysis with Bonferroni correction was used to generate adjusted P values, \* < 0.05, \*\* < 0.01,  
614 \*\*\*\* < 0.0001.

615

616 **Figure 3.** ELF3 orthologs suppress time to flowering of *elf3-2*. 12 wild type, *elf3-2* mutant,  
617 AtELF3 *elf3-2*, BdELF3 *elf3-2*, and SvELF3 *elf3-2* seedlings from two independent  
618 transformations were measured for days (A) and number of rosette leaves (B) at flowering (1 cm  
619 inflorescence). Mean and 95% confidence intervals are plotted as crosshairs. This experiment  
620 was repeated twice with similar results. ANOVA analysis with Bonferroni correction was used to  
621 generate adjusted P values, \*\* < 0.01, \*\*\* < 0.001, \*\*\*\* < 0.0001, of measurements when  
622 compared to the *elf3-2* mutant line.

623

624 **Figure 4.** ELF3 orthologs can recover *CCA1::LUC* rhythms and amplitude in *elf3-2* mutants. 8  
625 seedlings of wild type, *elf3-2* mutant, AtELF3 *elf3-2* (A), BdELF3 *elf3-2* (B), and SvELF3 *elf3-2*  
626 (C) from two independent transformations were imaged for bioluminescence under constant light  
627 after entrainment in 12-hour light :12-hour dark growth conditions at 22 °C. Each plot shows

628 average bioluminescence of all seedlings along with 95% confidence interval (error bars). This  
629 experiment was repeated four times with similar results. Note that wild type and *elf3-2* mutant  
630 data was plotted on all graphs for comparison. **(D)** Periods of seedlings. Only periods with a  
631 Relative Amplitude Error below 0.5 (see **Supplemental Figure S7**) were plotted. Mean and 95%  
632 confidence intervals are plotted as crosshairs. ANOVA analysis with Bonferroni correction was  
633 used to generate adjusted P values, \* < 0.05, \*\* < 0.01, \*\*\* < 0.001, \*\*\*\* < 0.0001, of  
634 measurements when compared to the wild type.

635

636 **Figure 5.** Both BdELF3 and SvELF3 can directly bind to AtELF4 and AtLUX. Yeast two-hybrid  
637 analysis of testing if either BdELF3 **(A)** or SvELF3 **(B)** can directly interact with either AtELF4,  
638 the N-terminal half of AtLUX (AtLUX-N, a.a. 1-143) or the C-terminal half of AtLUX (AtLUX-  
639 C, a.a. 144-324). –LW tests for the presence of both bait (DBD) and pray (AD) vectors, while the  
640 –LWH + 3AT tests for interaction. Vector alone serves as interaction control. This experiment  
641 was repeated twice with similar results.

642

643

644

## 645 REFERENCES

646

- 647 Altschul, S.F., Gish, W., Miller, W., Myers, E.W., and Lipman, D.J. (1990). Basic local alignment  
648 search tool. *J Mol Biol* 215, 403-410.
- 649 Anwer, M.U., Boikoglou, E., Herrero, E., Hallstein, M., Davis, A.M., Velikkakam James, G., Nagy,  
650 F., and Davis, S.J. (2014). Natural variation reveals that intracellular distribution of ELF3 protein  
651 is associated with function in the circadian clock. *Elife* 3.
- 652 Barrett, T., Wilhite, S.E., Ledoux, P., Evangelista, C., Kim, I.F., Tomashevsky, M., Marshall, K.A.,  
653 Phillippy, K.H., Sherman, P.M., Holko, M., *et al.* (2013). NCBI GEO: archive for functional  
654 genomics data sets--update. *Nucleic Acids Res* 41, D991-995.
- 655 Bell-Pedersen, D., Cassone, V.M., Earnest, D.J., Golden, S.S., Hardin, P.E., Thomas, T.L., and  
656 Zoran, M.J. (2005). Circadian rhythms from multiple oscillators: lessons from diverse organisms.  
657 *Nat Rev Genet* 6, 544-556.
- 658 Bendix, C., Marshall, C.M., and Harmon, F.G. (2015). Circadian Clock Genes Universally Control  
659 Key Agricultural Traits. *Mol Plant* 8, 1135-1152.

660 Bennetzen, J.L., Schmutz, J., Wang, H., Percifield, R., Hawkins, J., Pontaroli, A.C., Estep, M., Feng,  
661 L., Vaughn, J.N., Grimwood, J., *et al.* (2012). Reference genome sequence of the model plant  
662 *Setaria*. *Nat Biotechnol* **30**, 555-561.

663 Boikoglou, E., Ma, Z., von Korff, M., Davis, A.M., Nagy, F., and Davis, S.J. (2011). Environmental  
664 memory from a circadian oscillator: the *Arabidopsis thaliana* clock differentially integrates  
665 perception of photic vs. thermal entrainment. *Genetics* **189**, 655-664.

666 Bray, N.L., Pimentel, H., Melsted, P., and Pachter, L. (2016). Near-optimal probabilistic RNA-seq  
667 quantification. *Nat Biotech* **34**, 525-527.

668 Brutnell, T.P., Wang, L., Swartwood, K., Goldschmidt, A., Jackson, D., Zhu, X.G., Kellogg, E., and  
669 Van Eck, J. (2010). *Setaria viridis*: a model for C4 photosynthesis. *Plant Cell* **22**, 2537-2544.

670 Bushnell, B. (2016). BBMap short read aligner. University of California, Berkeley, California URL  
671 <http://sourceforge.net/projects/bbmap>.

672 Calixto, C.P., Waugh, R., and Brown, J.W. (2015). Evolutionary relationships among barley and  
673 *Arabidopsis* core circadian clock and clock-associated genes. *J Mol Evol* **80**, 108-119.

674 Covington, M.F., Maloof, J.N., Straume, M., Kay, S.A., and Harmer, S.L. (2008). Global  
675 transcriptome analysis reveals circadian regulation of key pathways in plant growth and  
676 development. *Genome Biol* **9**, R130.

677 Covington, M.F., Panda, S., Liu, X.L., Strayer, C.A., Wagner, D.R., and Kay, S.A. (2001). ELF3  
678 modulates resetting of the circadian clock in *Arabidopsis*. *Plant Cell* **13**, 1305-1315.

679 Dixon, L.E., Knox, K., Kozma-Bognar, L., Southern, M.M., Pokhilko, A., and Millar, A.J. (2011).  
680 Temporal repression of core circadian genes is mediated through EARLY FLOWERING 3 in  
681 *Arabidopsis*. *Curr Biol* **21**, 120-125.

682 Dodd, A.N., Salathia, N., Hall, A., Kevei, E., Toth, R., Nagy, F., Hibberd, J.M., Millar, A.J., and  
683 Webb, A.A. (2005). Plant circadian clocks increase photosynthesis, growth, survival, and  
684 competitive advantage. *Science* **309**, 630-633.

685 Doherty, C.J., and Kay, S.A. (2010). Circadian control of global gene expression patterns. *Annu*  
686 *Rev Genet* **44**, 419-444.

687 Doyle, M.R., Davis, S.J., Bastow, R.M., McWatters, H.G., Kozma-Bognar, L., Nagy, F., Millar, A.J.,  
688 and Amasino, R.M. (2002). The ELF4 gene controls circadian rhythms and flowering time in  
689 *Arabidopsis thaliana*. *Nature* **419**, 74-77.

690 Edelstein, A., Amodaj, N., Hoover, K., Vale, R., and Stuurman, N. (2010). Computer control of  
691 microscopes using microManager. *Curr Protoc Mol Biol Chapter 14*, Unit14 20.

692 Edelstein, A.D., Tsuchida, M.A., Amodaj, N., Pinkard, H., Vale, R.D., and Stuurman, N. (2014).  
693 Advanced methods of microscope control using muManager software. *J Biol Methods* **1**.

694 Edgar, R., Domrachev, M., and Lash, A.E. (2002). Gene Expression Omnibus: NCBI gene  
695 expression and hybridization array data repository. *Nucleic Acids Res* **30**, 207-210.

696 Edgar, R.S., Green, E.W., Zhao, Y., van Ooijen, G., Olmedo, M., Qin, X., Xu, Y., Pan, M.,  
697 Valekunja, U.K., Feeney, K.A., *et al.* (2012). Peroxiredoxins are conserved markers of circadian  
698 rhythms. *Nature* **485**, 459-464.

699 Faure, S., Turner, A.S., Gruszka, D., Christodoulou, V., Davis, S.J., von Korff, M., and Laurie, D.A.  
700 (2012). Mutation at the circadian clock gene EARLY MATURITY 8 adapts domesticated barley  
701 (*Hordeum vulgare*) to short growing seasons. *Proc Natl Acad Sci U S A* **109**, 8328-8333.

702 Filichkin, S.A., Breton, G., Priest, H.D., Dharmawardhana, P., Jaiswal, P., Fox, S.E., Michael, T.P.,  
703 Chory, J., Kay, S.A., and Mockler, T.C. (2011). Global profiling of rice and poplar transcriptomes  
704 highlights key conserved circadian-controlled pathways and cis-regulatory modules. *PLoS One*  
705 *6*, e16907.

706 Goodstein, D.M., Shu, S., Howson, R., Neupane, R., Hayes, R.D., Fazo, J., Mitros, T., Dirks, W.,  
707 Hellsten, U., Putnam, N., *et al.* (2012). Phytozome: a comparative platform for green plant  
708 genomics. *Nucleic Acids Res* *40*, D1178-1186.

709 Gould, P.D., Diaz, P., Hogben, C., Kusakina, J., Salem, R., Hartwell, J., and Hall, A. (2009). Delayed  
710 fluorescence as a universal tool for the measurement of circadian rhythms in higher plants.  
711 *Plant J* *58*, 893-901.

712 Graf, A., Schlereth, A., Stitt, M., and Smith, A.M. (2010). Circadian control of carbohydrate  
713 availability for growth in Arabidopsis plants at night. *Proc Natl Acad Sci U S A* *107*, 9458-9463.

714 Greenham, K., and McClung, C.R. (2015). Integrating circadian dynamics with physiological  
715 processes in plants. *Nat Rev Genet* *16*, 598-610.

716 Harmer, S.L. (2009). The circadian system in higher plants. *Annu Rev Plant Biol* *60*, 357-377.

717 Harmer, S.L., Hogenesch, J.B., Straume, M., Chang, H.S., Han, B., Zhu, T., Wang, X., Kreps, J.A.,  
718 and Kay, S.A. (2000). Orchestrated transcription of key pathways in Arabidopsis by the circadian  
719 clock. *Science* *290*, 2110-2113.

720 Hazen, S.P., Schultz, T.F., Pruneda-Paz, J.L., Borevitz, J.O., Ecker, J.R., and Kay, S.A. (2005). LUX  
721 ARRHYTHMO encodes a Myb domain protein essential for circadian rhythms. *Proc Natl Acad Sci*  
722 *U S A* *102*, 10387-10392.

723 Helfer, A., Nusinow, D.A., Chow, B.Y., Gehrke, A.R., Bulyk, M.L., and Kay, S.A. (2011). LUX  
724 ARRHYTHMO encodes a nighttime repressor of circadian gene expression in the Arabidopsis  
725 core clock. *Curr Biol* *21*, 126-133.

726 Herrero, E., Kolmos, E., Bujdosó, N., Yuan, Y., Wang, M., Berns, M.C., Uhlworm, H., Coupland,  
727 G., Saini, R., Jaskolski, M., *et al.* (2012). EARLY FLOWERING4 recruitment of EARLY FLOWERING3  
728 in the nucleus sustains the Arabidopsis circadian clock. *Plant Cell* *24*, 428-443.

729 Hicks, K.A., Albertson, T.M., and Wagner, D.R. (2001). EARLY FLOWERING3 encodes a novel  
730 protein that regulates circadian clock function and flowering in Arabidopsis. *Plant Cell* *13*, 1281-  
731 1292.

732 Hicks, K.A., Millar, A.J., Carre, I.A., Somers, D.E., Straume, M., Meeks-Wagner, D.R., and Kay,  
733 S.A. (1996). Conditional circadian dysfunction of the Arabidopsis early-flowering 3 mutant.  
734 *Science* *274*, 790-792.

735 Higgins, J.A., Bailey, P.C., and Laurie, D.A. (2010). Comparative genomics of flowering time  
736 pathways using *Brachypodium distachyon* as a model for the temperate grasses. *PLoS One* *5*,  
737 e10065.

738 Hsu, P.Y., and Harmer, S.L. (2014). Wheels within wheels: the plant circadian system. *Trends in*  
739 *plant science* *19*, 240-249.

740 Huang, H., Alvarez, S., Bindbeutel, R., Shen, Z., Naldrett, M.J., Evans, B.S., Briggs, S.P., Hicks,  
741 L.M., Kay, S.A., and Nusinow, D.A. (2016a). Identification of Evening Complex Associated  
742 Proteins in Arabidopsis by Affinity Purification and Mass Spectrometry. *Mol Cell Proteomics* *15*,  
743 201-217.

744 Huang, H., Alvarez, S., and Nusinow, D.A. (2016b). Data on the identification of protein  
745 interactors with the Evening Complex and PCH1 in Arabidopsis using tandem affinity  
746 purification and mass spectrometry (TAP-MS). *Data Brief* 8, 56-60.

747 Huang, H., and Nusinow, D. (2016a). Tandem Purification of His6-3x FLAG Tagged Proteins for  
748 Mass Spectrometry from Arabidopsis. *Bio-Protocol* 6.

749 Huang, H., and Nusinow, D.A. (2016b). Into the Evening: Complex Interactions in the  
750 Arabidopsis Circadian Clock. *Trends Genet* 32, 674-686.

751 Huang, H., Yoo, C.Y., Bindbeutel, R., Goldsworthy, J., Tielking, A., Alvarez, S., Naldrett, M.J.,  
752 Evans, B.S., Chen, M., and Nusinow, D.A. (2016c). PCH1 integrates circadian and light-signaling  
753 pathways to control photoperiod-responsive growth in Arabidopsis. *eLife* 5, e13292.

754 Hughes, M.E., Hogenesch, J.B., and Kornacker, K. (2010). JTK\_CYCLE: an efficient nonparametric  
755 algorithm for detecting rhythmic components in genome-scale data sets. *J Biol Rhythms* 25,  
756 372-380.

757 Keller, A., Nesvizhskii, A.I., Kolker, E., and Aebersold, R. (2002). Empirical Statistical Model To  
758 Estimate the Accuracy of Peptide Identifications Made by MS/MS and Database Search.  
759 *Analytical Chemistry* 74, 5383-5392.

760 Khan, S., Rowe, S.C., and Harmon, F.G. (2010). Coordination of the maize transcriptome by a  
761 conserved circadian clock. *BMC Plant Biol* 10, 126.

762 Khanna, R., Kikis, E.A., and Quail, P.H. (2003). EARLY FLOWERING 4 functions in phytochrome B-  
763 regulated seedling de-etiolation. *Plant Physiol* 133, 1530-1538.

764 Kim, W.Y., Hicks, K.A., and Somers, D.E. (2005). Independent roles for EARLY FLOWERING 3 and  
765 ZEITLUPE in the control of circadian timing, hypocotyl length, and flowering time. *Plant Physiol*  
766 139, 1557-1569.

767 Kolmos, E., Herrero, E., Bujdoso, N., Millar, A.J., Toth, R., Gyula, P., Nagy, F., and Davis, S.J.  
768 (2011). A reduced-function allele reveals that EARLY FLOWERING3 repressive action on the  
769 circadian clock is modulated by phytochrome signals in Arabidopsis. *Plant Cell* 23, 3230-3246.

770 Kumar, R., Ichihashi, Y., Kimura, S., Chitwood, D.H., Headland, L.R., Peng, J., Maloof, J.N., and  
771 Sinha, N.R. (2012). A High-Throughput Method for Illumina RNA-Seq Library Preparation. *Front*  
772 *Plant Sci* 3, 202.

773 Liu, X.L., Covington, M.F., Fankhauser, C., Chory, J., and Wagner, D.R. (2001). ELF3 encodes a  
774 circadian clock-regulated nuclear protein that functions in an Arabidopsis PHYB signal  
775 transduction pathway. *Plant Cell* 13, 1293-1304.

776 Lou, P., Wu, J., Cheng, F., Cressman, L.G., Wang, X., and McClung, C.R. (2012). Preferential  
777 retention of circadian clock genes during diploidization following whole genome triplication in  
778 *Brassica rapa*. *Plant Cell* 24, 2415-2426.

779 Lu, S., Zhao, X., Hu, Y., Liu, S., Nan, H., Li, X., Fang, C., Cao, D., Shi, X., Kong, L., *et al.* (2017).  
780 Natural variation at the soybean J locus improves adaptation to the tropics and enhances yield.  
781 *Nat Genet*.

782 Matos, D.A., Cole, B.J., Whitney, I.P., MacKinnon, K.J., Kay, S.A., and Hazen, S.P. (2014). Daily  
783 changes in temperature, not the circadian clock, regulate growth rate in *Brachypodium*  
784 *distachyon*. *PLoS One* 9, e100072.

785 Matsubara, K., Ogiso-Tanaka, E., Hori, K., Ebana, K., Ando, T., and Yano, M. (2012). Natural  
786 variation in Hd17, a homolog of Arabidopsis ELF3 that is involved in rice photoperiodic  
787 flowering. *Plant Cell Physiol* 53, 709-716.

788 McClung, C.R. (2013). Beyond Arabidopsis: the circadian clock in non-model plant species.  
789 *Semin Cell Dev Biol* 24, 430-436.

790 Michael, T.P., Mockler, T.C., Breton, G., McEntee, C., and Byer, A. (2008). Network discovery  
791 pipeline elucidates conserved time-of-day-specific cis-regulatory modules. *PLoS genetics*.

792 Michael, T.P., Salome, P.A., and McClung, C.R. (2003). Two Arabidopsis circadian oscillators can  
793 be distinguished by differential temperature sensitivity. *Proc Natl Acad Sci U S A* 100, 6878-  
794 6883.

795 Mizuno, T., Nomoto, Y., Oka, H., Kitayama, M., Takeuchi, A., Tsubouchi, M., and Yamashino, T.  
796 (2014). Ambient temperature signal feeds into the circadian clock transcriptional circuitry  
797 through the EC night-time repressor in Arabidopsis thaliana. *Plant Cell Physiol* 55, 958-976.

798 Mockler, T.C., Michael, T.P., Priest, H.D., Shen, R., Sullivan, C.M., Givan, S.A., McEntee, C., Kay,  
799 S.A., and Chory, J. (2007). The DIURNAL project: DIURNAL and circadian expression profiling,  
800 model-based pattern matching, and promoter analysis. *Cold Spring Harb Symp Quant Biol* 72,  
801 353-363.

802 Murakami, M., Ashikari, M., Miura, K., Yamashino, T., and Mizuno, T. (2003). The Evolutionarily  
803 Conserved OsPRR Quintet: Rice Pseudo-Response Regulators Implicated in Circadian Rhythm.  
804 *Plant and Cell Physiology* 44, 1229-1236.

805 Nagel, D.H., and Kay, S.A. (2012). Complexity in the wiring and regulation of plant circadian  
806 networks. *Curr Biol* 22, R648-657.

807 Nesvizhskii, A.I., Keller, A., Kolker, E., and Aebersold, R. (2003). A Statistical Model for  
808 Identifying Proteins by Tandem Mass Spectrometry. *Analytical Chemistry* 75, 4646-4658.

809 Nozue, K., Covington, M.F., Duek, P.D., Lorrain, S., Fankhauser, C., Harmer, S.L., and Maloof, J.N.  
810 (2007). Rhythmic growth explained by coincidence between internal and external cues. *Nature*  
811 448, 358-361.

812 Nusinow, D.A., Helfer, A., Hamilton, E.E., King, J.J., Imaizumi, T., Schultz, T.F., Farre, E.M., and  
813 Kay, S.A. (2011). The ELF4-ELF3-LUX complex links the circadian clock to diurnal control of  
814 hypocotyl growth. *Nature* 475, 398-402.

815 Onai, K., and Ishiura, M. (2005). PHYTOCLOCK 1 encoding a novel GARP protein essential for the  
816 Arabidopsis circadian clock. *Genes Cells* 10, 963-972.

817 Ouyang, Y., Andersson, C.R., Kondo, T., Golden, S.S., and Johnson, C.H. (1998). Resonating  
818 circadian clocks enhance fitness in cyanobacteria. *Proc Natl Acad Sci U S A* 95, 8660-8664.

819 Plautz, J.D., Straume, M., Stanewsky, R., Jamison, C.F., Brandes, C., Dowse, H.B., Hall, J.C., and  
820 Kay, S.A. (1997). Quantitative Analysis of Drosophila period Gene Transcription in Living  
821 Animals. *Journal of Biological Rhythms* 12, 204-217.

822 Poire, R., Wiese-Klinkenberg, A., Parent, B., Mielewicz, M., Schurr, U., Tardieu, F., and Walter,  
823 A. (2010). Diel time-courses of leaf growth in monocot and dicot species: endogenous rhythms  
824 and temperature effects. *J Exp Bot* 61, 1751-1759.



825 Pokhilko, A., Fernandez, A.P., Edwards, K.D., Southern, M.M., Halliday, K.J., and Millar, A.J.  
826 (2012). The clock gene circuit in Arabidopsis includes a repressilator with additional feedback  
827 loops. *Mol Syst Biol* 8, 574.

828 Pruneda-Paz, J.L., Breton, G., Para, A., and Kay, S.A. (2009). A functional genomics approach  
829 reveals CHE as a component of the Arabidopsis circadian clock. *Science* 323, 1481-1485.

830 Saito, H., Ogiso-Tanaka, E., Okumoto, Y., Yoshitake, Y., Izumi, H., Yokoo, T., Matsubara, K., Hori,  
831 K., Yano, M., Inoue, H., *et al.* (2012). E7 encodes an ELF3-like protein and promotes rice  
832 flowering by negatively regulating the floral repressor gene *Ghd7* under both short- and long-  
833 day conditions. *Plant Cell Physiol* 53, 717-728.

834 Sakuraba, Y., Han, S.H., Yang, H.J., Piao, W., and Paek, N.C. (2016). Mutation of Rice Early  
835 Flowering3.1 (*OsELF3.1*) delays leaf senescence in rice. *Plant Mol Biol*.

836 Sakuraba, Y., Jeong, J., Kang, M.Y., Kim, J., Paek, N.C., and Choi, G. (2014). Phytochrome-  
837 interacting transcription factors PIF4 and PIF5 induce leaf senescence in Arabidopsis. *Nat*  
838 *Commun* 5, 4636.

839 Schneider, C.A., Rasband, W.S., and Eliceiri, K.W. (2012). NIH Image to ImageJ: 25 years of  
840 image analysis. *Nat Meth* 9, 671-675.

841 Shor, E., and Green, R.M. (2016). The Impact of Domestication on the Circadian Clock. *Trends*  
842 *Plant Sci* 21, 281-283.

843 Sievers, F., Wilm, A., Dineen, D., Gibson, T.J., Karplus, K., Li, W., Lopez, R., McWilliam, H.,  
844 Remmert, M., Soding, J., *et al.* (2011). Fast, scalable generation of high-quality protein multiple  
845 sequence alignments using Clustal Omega. *Mol Syst Biol* 7, 539.

846 Song, Y.H., Ito, S., and Imaizumi, T. (2010). Similarities in the circadian clock and  
847 photoperiodism in plants. *Curr Opin Plant Biol* 13, 594-603.

848 Song, Y.H., Shim, J.S., Kinmonth-Schultz, H.A., and Imaizumi, T. (2014). Photoperiodic Flowering:  
849 Time Measurement Mechanisms in Leaves. *Annu Rev Plant Biol*.

850 Van Leene, J., Eeckhout, D., Cannoot, B., De Winne, N., Persiau, G., Van De Slijke, E., Vercruyse,  
851 L., Dedecker, M., Verkest, A., Vandepoele, K., *et al.* (2015). An improved toolbox to unravel the  
852 plant cellular machinery by tandem affinity purification of Arabidopsis protein complexes. *Nat*  
853 *Protocols* 10, 169-187.

854 Vizcaino, J.A., Deutsch, E.W., Wang, R., Csordas, A., Reisinger, F., Rios, D., Dienes, J.A., Sun, Z.,  
855 Farrah, T., Bandeira, N., *et al.* (2014). ProteomeXchange provides globally coordinated  
856 proteomics data submission and dissemination. *Nat Biotechnol* 32, 223-226.

857 Wang, L., Si, Y., Dedow, L.K., Shao, Y., Liu, P., and Brutnell, T.P. (2011a). A low-cost library  
858 construction protocol and data analysis pipeline for Illumina-based strand-specific multiplex  
859 RNA-seq. *PLoS One* 6, e26426.

860 Wang, W., Barnaby, J.Y., Tada, Y., Li, H., Tor, M., Caldelari, D., Lee, D.U., Fu, X.D., and Dong, X.  
861 (2011b). Timing of plant immune responses by a central circadian regulator. *Nature* 470, 110-  
862 114.

863 Wang, Z., Casas-Mollano, J.A., Xu, J., Riethoven, J.J., Zhang, C., and Cerutti, H. (2015). Osmotic  
864 stress induces phosphorylation of histone H3 at threonine 3 in pericentromeric regions of  
865 Arabidopsis thaliana. *Proc Natl Acad Sci U S A* 112, 8487-8492.

866 Weller, J.L., Liew, L.C., Hecht, V.F.G., Rajandran, V., Laurie, R.E., Ridge, S., Wenden, B., Vander  
867 Schoor, J.K., Jaminon, O., Blassiau, C., *et al.* (2012). A conserved molecular basis for  
868 photoperiod adaptation in two temperate legumes. *Proc Natl Acad Sci U S A* *109*, 21158-21163.  
869 Wijnen, H., and Young, M.W. (2006). Interplay of circadian clocks and metabolic rhythms. *Annu*  
870 *Rev Genet* *40*, 409-448.  
871 Woelfle, M.A., Ouyang, Y., Phanvijhitsiri, K., and Johnson, C.H. (2004). The adaptive value of  
872 circadian clocks: an experimental assessment in cyanobacteria. *Curr Biol* *14*, 1481-1486.  
873 Wu, J.F., Wang, Y., and Wu, S.H. (2008). Two new clock proteins, LWD1 and LWD2, regulate  
874 *Arabidopsis* photoperiodic flowering. *Plant Physiol* *148*, 948-959.  
875 Yang, Y., Peng, Q., Chen, G.-X., Li, X.-H., and Wu, C.-Y. (2013). OsELF3 is involved in circadian  
876 clock regulation for promoting flowering under long-day conditions in rice. *Mol Plant* *6*, 202-  
877 215.  
878 Yu, J.W., Rubio, V., Lee, N.Y., Bai, S., Lee, S.Y., Kim, S.S., Liu, L., Zhang, Y., Irigoyen, M.L., Sullivan,  
879 J.A., *et al.* (2008). COP1 and ELF3 control circadian function and photoperiodic flowering by  
880 regulating GI stability. *Mol Cell* *32*, 617-630.  
881 Zagotta, M., Shannon, S., Jacobs, C., and Meeks-Wagner, D. (1992). Early-Flowering Mutants of  
882 *Arabidopsis thaliana*. *Functional Plant Biology* *19*, 411-418.  
883 Zakhrabekova, S., Gough, S.P., Braumann, I., Muller, A.H., Lundqvist, J., Ahmann, K., Dockter, C.,  
884 Matyszczyk, I., Kurowska, M., Druka, A., *et al.* (2012). Induced mutations in circadian clock  
885 regulator Mat-a facilitated short-season adaptation and range extension in cultivated barley.  
886 *Proc Natl Acad Sci U S A* *109*, 4326-4331.  
887 Zhang, X., Henriques, R., Lin, S.-S., Niu, Q.-W., and Chua, N.-H. (2006). Agrobacterium-mediated  
888 transformation of *Arabidopsis thaliana* using the floral dip method. *Nat Protocols* *1*, 641-646.  
889 Zhao, J., Huang, X., Ouyang, X., Chen, W., Du, A., Zhu, L., Wang, S., Deng, X.W., and Li, S. (2012).  
890 OsELF3-1, an ortholog of *Arabidopsis* early flowering 3, regulates rice circadian rhythm and  
891 photoperiodic flowering. *PLoS One* *7*, e43705.  
892 Zhu, D., Maier, A., Lee, J.H., Laubinger, S., Saijo, Y., Wang, H., Qu, L.J., Hoecker, U., and Deng,  
893 X.W. (2008). Biochemical characterization of *Arabidopsis* complexes containing  
894 CONSTITUTIVELY PHOTOMORPHOGENIC1 and SUPPRESSOR OF PHYA proteins in light control of  
895 plant development. *Plant Cell* *20*, 2307-2323.  
896

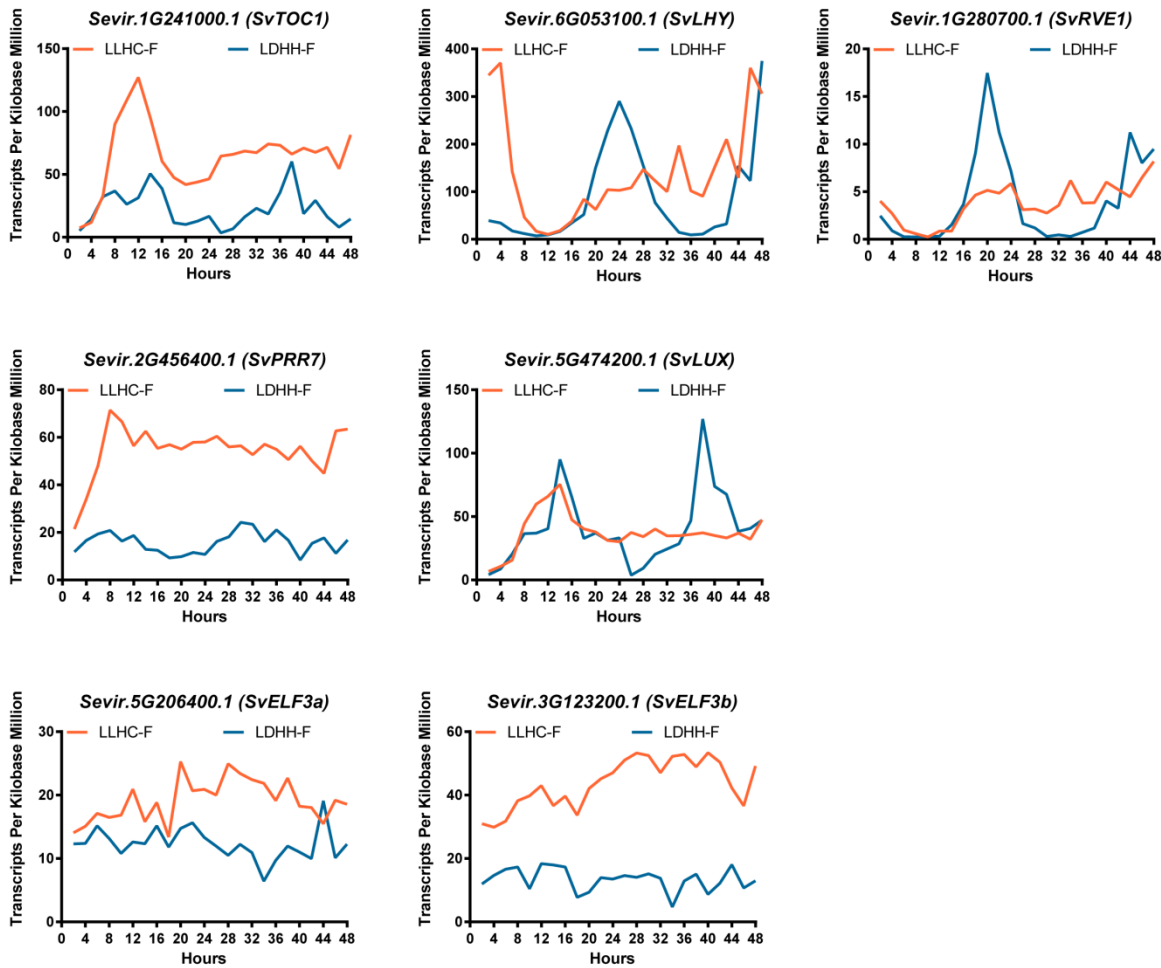


**Figure 1.** Circadian expression profiles of putative *S. viridis* clock components from Diel Explorer using time-course RNA-seq data. *S. viridis* plants were entrained by either photocycle (LDHH) or thermocycle (LLHC), followed by being sampled every 2 hours for 48 hours under constant temperature and light conditions (Free-Running; F) to generate time-course RNA-seq data. Mean values of Transcripts per Kilobase Million (TPM) from two experimental replicates for each timepoints per gene were plotted.

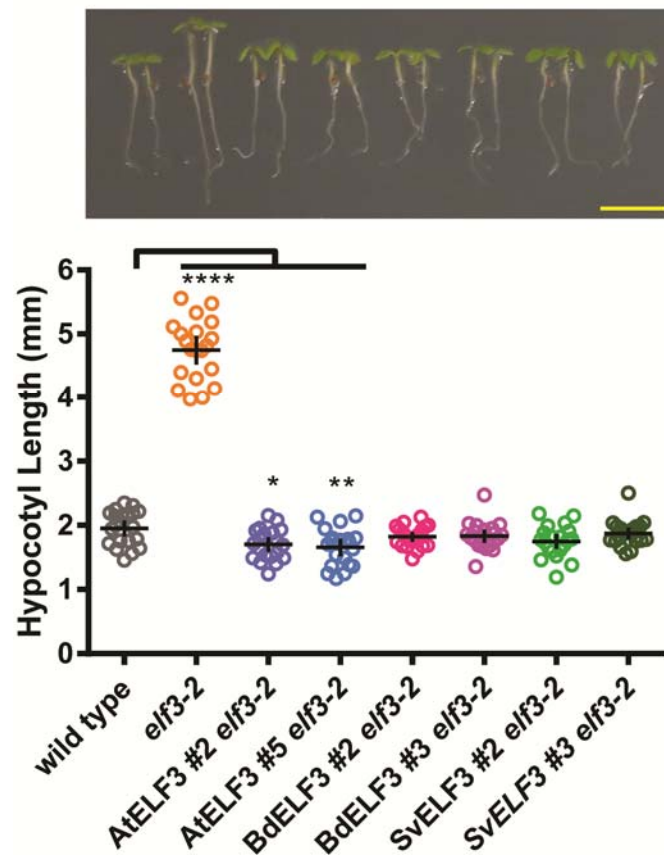


**Figure 2.** ELF3 orthologs suppress hypocotyl elongation defects in *elf3-2*. The hypocotyls of 20 seedlings of wild type, *elf3-2* mutant, AtELF3 *elf3-2*, BdELF3 *elf3-2*, and SvELF3 *elf3-2* (two independent transgenic lines for each ELF3 ortholog) were measured at 4 days after germination under 12-hour light :12-hour dark growth conditions at 22 °C. Upper panel shows representative seedlings of each genotype, with scale bar equal to 5 mm. Mean and 95% confidence intervals are plotted as crosshairs. This experiment was repeated three times with similar results. ANOVA analysis with Bonferroni correction was used to generate adjusted P values, \* < 0.05, \*\* < 0.01, \*\*\*\* < 0.0001.

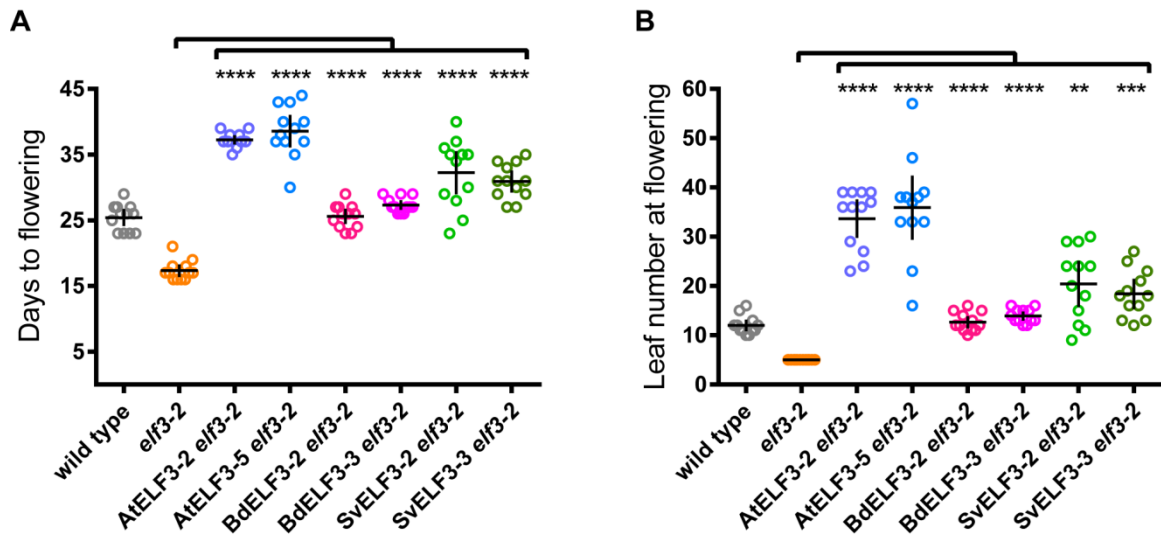


**Figure 3.** ELF3 orthologs suppress time to flowering of *elf3-2*. 12 wild type, *elf3-2* mutant, AtELF3 *elf3-2*, BdELF3 *elf3-2*, and SvELF3 *elf3-2* seedlings from two independent transformations were measured for days (A) and number of rosette leaves (B) at flowering (1 cm inflorescence). Mean and 95% confidence intervals are plotted as crosshairs. This experiment was repeated twice with similar results. ANOVA analysis with Bonferroni correction was used to generate adjusted P values, \*\* < 0.01, \*\*\* < 0.001, \*\*\*\* < 0.0001, of measurements when compared to the *elf3-2* mutant line.

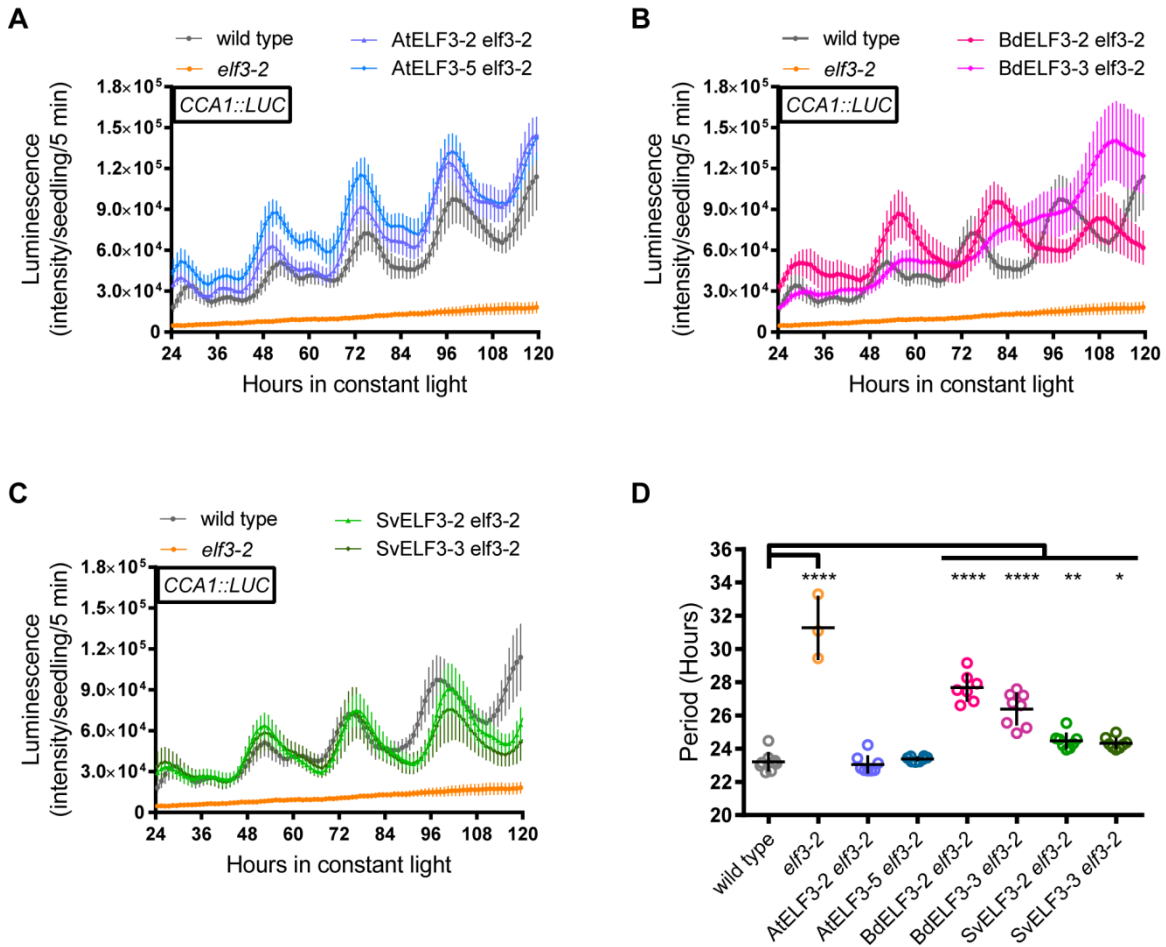


**Figure 4.** ELF3 orthologs can recover *CCA1::LUC* rhythms and amplitude in *elf3-2* mutants. 8 seedlings of wild type, *elf3-2* mutant, AtELF3 *elf3-2* (A), BdELF3 *elf3-2* (B), and SvELF3 *elf3-2* (C) from two independent transformations were imaged for bioluminescence under constant light after entrainment in 12-hour light :12-hour dark growth conditions at 22 °C. Each plot shows average bioluminescence of all seedlings along with 95% confidence interval (error bars). This experiment was repeated four times with similar results. Note that wild type and *elf3-2* mutant data was plotted on all graphs for comparison. (D) Periods of seedlings. Only periods with a Relative Amplitude Error below 0.5 (see **Supplemental Figure S7**) were plotted. Mean and 95% confidence intervals are plotted as crosshairs. ANOVA analysis with Bonferroni correction was used to generate adjusted P values, \* < 0.05, \*\* < 0.01, \*\*\* < 0.001, \*\*\*\* < 0.0001, of measurements when compared to the wild type.

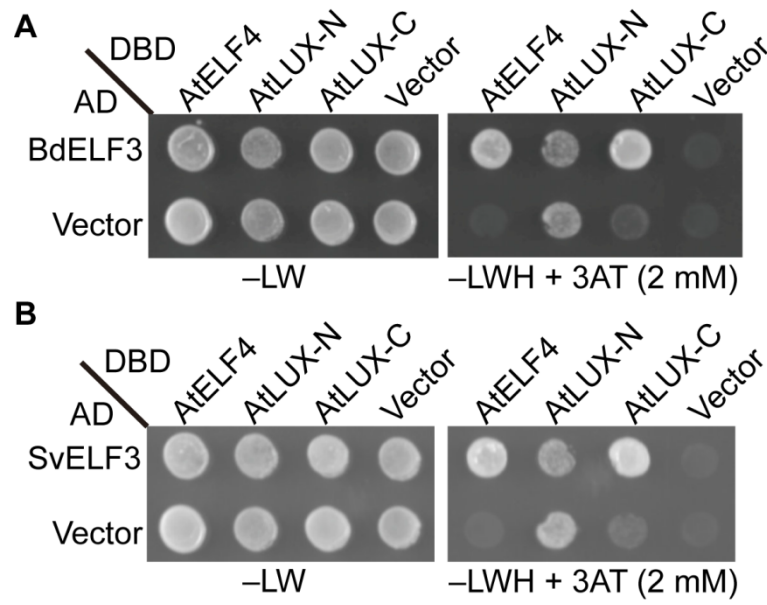


**Figure 5.** Both BdELF3 and SvELF3 can directly bind to AtELF4 and AtLUX. Yeast two-hybrid analysis of testing if either BdELF3 (**A**) or SvELF3 (**B**) can directly interact with either AtELF4, the N-terminal half of AtLUX (AtLUX-N, a.a. 1-143) or the C-terminal half of AtLUX (AtLUX-C, a.a. 144-324). -LW tests for the presence of both bait (DBD) and prey (AD) vectors, while the -LWH + 3AT tests for interaction. Vector alone serves as interaction control. This experiment was repeated twice with similar results.